INTERNATIONAL JOURNAL FOR NUMERICAL AND ANALYTICAL METHODS IN GEOMECHANICS
Int. J. Numer. Anal. Meth. Geomech., **23**, 1909–1926 (1999)

SELECTION OF *p–y* CURVES FOR THE DESIGN OF SINGLE LATERALLY LOADED PILES

M. F. BRANSBY*

Centre for Offshore Foundation Systems, University of Western Australia, Nedlands, WA 6907, Australia

Two-dimensional finite element analysis has been used to find load–transfer relationships for translation of an infinitely long pile through undrained soil for a variety of soil-constitutive models. It has been shown that these load–transfer curves can be used as *p–y* curves in the analysis of single piles undergoing lateral pile head loading in undrained soils with non-linear stress–strain laws. Lateral pile response deduced from 2-D analysis input to the subgrade reaction method has been compared to the behaviour of a single pile analysed using three-dimensional finite element analysis. Good agreement between the two methods for non-linear soils suggests that the 2-D analysis may form a useful design method for calculation of *p–y* curves. Copyright © 1999 John Wiley & Sons, Ltd.

KEY WORDS: lateral pile loading; subgrade reaction method; finite element analysis

INTRODUCTION

Although vertical piles are primarily designed to withstand vertical loading, they are often also subjected to lateral loads. This is particularly the case offshore where much research has been undertaken to understand the response of piles to lateral loading.[1–4] Serviceability design methods may be split into two categories: continuum methods and the subgrade reaction (or '*p–y*') method.

In the continuum method,[5,6] the soil is usually first idealized as a linear elastic material (with strain-independent stiffness) before elastic analysis is applied.[5] As soil is not linearly elastic, engineering judgement must be applied to obtain suitable elastic properties. This judgement must pre-suppose the approximate strain levels which vary with both pile displacement and position around the pile. Therefore, although, the method is not empirical in itself, choice of appropriate material parameters often is.

In the subgrade reaction method the soil is idealized as a series of usually non-linear springs relating pile pressure, p, to normalized pile displacement, y/d, where d is the pile diameter. The pile equilibrium equations assuming a linear elastic pile are solved for a given head loading and so the deflected pile shape and pressure and bending moment distribution is obtained. Many research workers have recommended different pressure–displacement ($p–y$) curves for varying soils[1,3] but most are based on empirical curve fitting of either full-scale field tests or centrifuge model tests.[7–9] Work has been attempted to relate the $p–y$ curves to fundamental soil properties (e.g. Reference 10), but the findings have been inconclusive. Emprically derived curves are normalized

*Correspondence to: Dr. Mark Fraser Bransby, Research Fellow, Centre for Offshore Foundation Systems, University of Western Australia, Nedlands, WA 6907, Australia. E-mail: fraser@civil.uwa.edu.au

CCC 0363–9061/99/151909–18$17.50

Received 4 February 1998
Revised 20 November 1998

by soil undrained shear strength or soil stiffness at a certain shear strain or proportion of mobilized shear stress[1], eg. E_{50}.

Load–transfer curves are often expressed in terms of P–y, where P is the pile load per unit length, and are known as *load*–transfer curves. In this paper, they are plotted in terms of pile pressure, p against normalized displacement, δ/d which is a direct scaling (by d) of the P–y form. However, this form has the advantage that normalized pile displacement (δ/d) is plotted which gives a better indication of expected strain levels in the soil. The gradient of both load–transfer forms will have units of modulus and this will relate to soil properties, e.g. the shear modulus, G. Additionally, the pile pressure can be normalized by a soil property (such as G or s_u) to make the plots dimensionless and generalizable.

As soil moves laterally past piles, or piles past soil, the development of lateral pile pressure due to the local soil behaviour can be analysed using a finite element study of a 2-D horizontal cross-section.[11,12] For this case, the pile displacement is defined as δ. However, the initial stiffness of the elastic p–δ response will depend on the distance of the rigid boundaries from the pile. Baguelin *et al.*[12] found that, in an undrained linear elastic circular space of radius R, the pile load–transfer curve could be expressed as

$$p = \frac{3}{s} G \left(\frac{\delta}{d} \right) \tag{1}$$

where $s = 0{\cdot}573 + 0{\cdot}239 \ln (R/15d)$. Hence, the stiffness of the load–transfer curve was largely dependent of the boundary distance (for $R = \infty$, stiffness is zero) and so use of the method would require recommendation of R. Following elastic analysis of various piles in elastic soil using the Mindlin[13] solution, Baguelin *et al.*[12] recommended values of R which would give appropriate p–y stiffnesses for load–transfer analysis. They found that different values of R were required for different pile head loading conditions and pile geometries.

Soil deformation mechanisms around piles and pile groups, which occur during lateral loading, and load–transfer curves (or p–δ curves) may be determined using 2-D analysis for soils with different constitutive laws.[14] Their use allows greater insight of the local soil deformation mechanisms occurring in the 3-D geometry of a real pile–soil system. In particular, the p–δ curves obtained using 2-D analysis should be compared with the p–y curves found from 3-D analysis of the whole system.

TWO-DIMENSIONAL FINITE ELEMENT ANALYSIS

The finite element package CRISP, CRItical State Programs[15,16] was used. Due to symmetry, only the region between the pile centre-line and the centre-line between piles in a row has to be modelled (Figure 1). In the analyses, 760 15 noded triangular elements with 27 degrees of freedom were employed, which assumed a linear distribution of pore pressure and a cubic distribution of strain across the element (cubic strain traingles).

The geometrical and load definitions used in this paper are summarized, in Figure 1.

A rigid disk of diameter $d = 2$ m representing the pile was translated a distance δ through a region of soil with boundaries, $R = 25$d from the pile centre in up to 400 equal increments (Figure 1). At the soil-disk interface, soil was constrained to move with the disk, preventing slip between the soil and disk. To ensure numerical stability a consolidation analysis was carried out. However, time steps were reduced so that the soil behaviour was virtually undrained and the soil

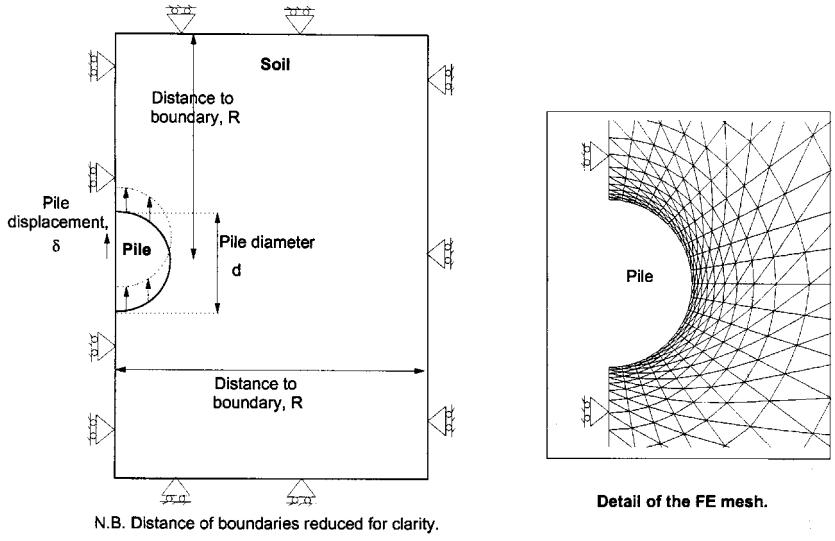

Figure 1. Geometry for 2-D finite element modelling

in the area of interest would have been incompressible. The behaviour of two types of soil will be reported here: linear elastic soil and power law soil. Both of these soil models have been used for the description of soil behaviour prior to failure, and so design methods based upon these models can only be used for prediction of undrained serviceability displacements.

Linear elastic soil

Linear elastic soil was used with shear modulus, G and Poisson's ratio, $v' = 0{\cdot}33$. Because the analyses were carried out effectively undrained, the soil would have behaved incompressibly and so the element behaviour would have been independent of the prescribed Poisson's ratio.

The stiffness of the pressure–displacement (p–δ) curve was found as $p = 4{\cdot}26\,\mathrm{G}\ (\delta/d)$. This compares well with the Baguelin *et al.*[12] exact solution of $p = 4{\cdot}32\,\mathrm{G}\ (\delta/d)$ with circular boundaries $25d$ from the pile centre. Therefore, Baguelin *et al.*'s equation (equation (1)) may also be used to give good approximation to the elastic stiffness of a pile in a *rectangular* space.

Power law soil

The undrained soil shear stress–shear strain law was described by the non-linearly elastic idealization

$$q_{\mathrm{mob}} = a\varepsilon_q^b \tag{2}$$

where q_{mob} is the mobilized deviatoric stress, ε_q is the deviatoric strain and a and b are soil constants. A small initial linear region (when $\varepsilon_q < 0{\cdot}0001$) was required to ensure that soil stiffness was not infinite at $\varepsilon_q = 0$.

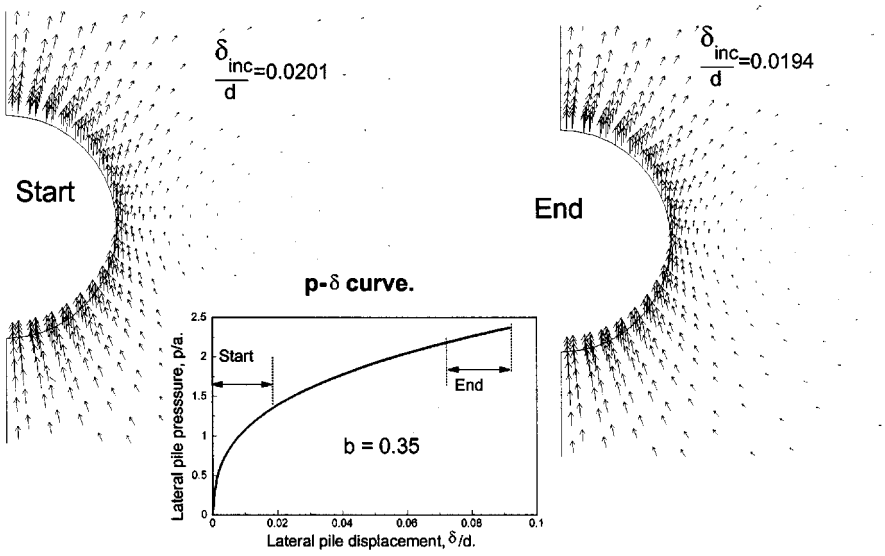

Figure 2. Soil deformation mechanisms for disk in power law soil

Examination of the soil deformation mechanisms at the beginning and end of pile translation (Figure 2) through soil with exponent $b = 0{\cdot}35$ reveals that the soil deformation mechanism is virtually unchanged throughout pile translation. The normalized p–δ curve produced (Figure 3) is of the same form as the shear stress–strain law. Indeed, a scaled version of the stress–strain law ($6{\cdot}15q/a$ against ε_q) is plotted on the same axis with an excellent agreement (Figure 3).

Bransby and Springman[14] examined analytically the behaviour of deformation mechanisms in power law soil, $q = a\varepsilon_q^b$. Using an energy-based approach they showed that a single deformation mechanism would prevail throughout displacement for a given geometry and power law exponent, b. This was largely due to the lack of characteristic strain in the power law soil model which allowed self-similar deformation to occur.[17] The system behaviour can be described using a simple scaling of the stress–strain law with a suitable value for the constant A in the equation below:

$$p = Aa\left(\frac{\delta}{d}\right)^b \tag{3}$$

For every different problem geometry and soil exponent there will be a single A value which can be used to obtain the load–transfer curve of the system from the stress–strain curve. For the fixed geometry of lateral translation of a single pile, knowledge of the relationship between A and b will allow estimation of the pile p–δ curve as soon as the power law of the soil is known.

Finite element results determining the A–b relationships for two separate boundary conditions, boundary distance, $R = 25$d and $R = 12{\cdot}5$d are shown in Figure 4.

The boundaries have a non-uniform effect on the A–b relationship over the range of b values as illustrated by the convergence of the two A–b relationships as b reduces. This effect is clarified in Figure 4 where the difference in A value between the analysis with $R/d = 25$ and $R/d = 12{\cdot}5$ is

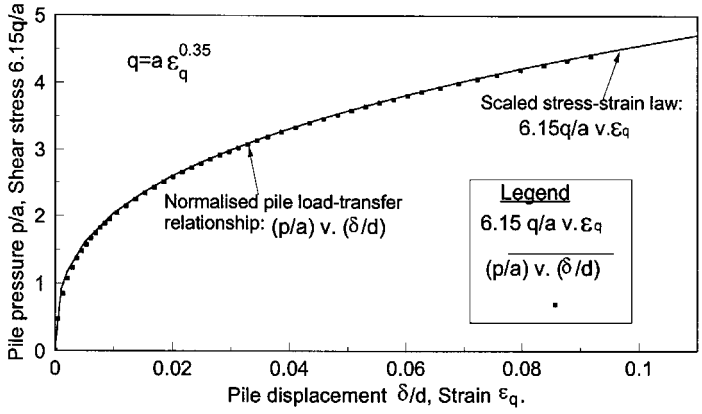

Figure 3. Load–transfer curve and stress–strain curve for disk translation through power-law soil

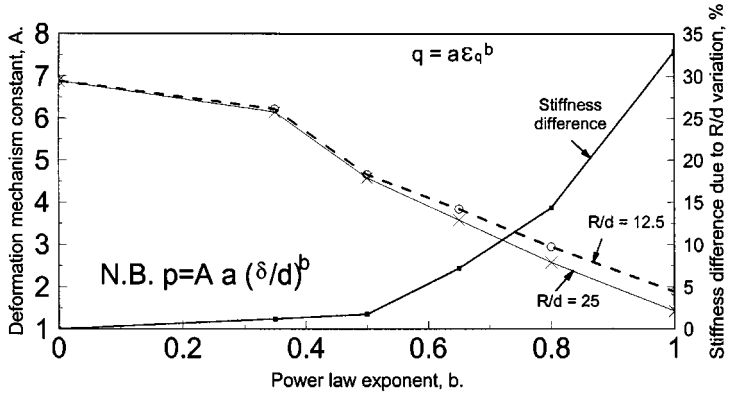

Figure 4. A–b relationship for the 2-D pile translation

plotted against b. Indeed, the Baguelin *et al.*[12] equation (1) shows that for linear elasticity (when $b = 1$ and $a = 3G$), A reduces as R increases. However, the plastic failure load (when $b = 0$ and $a = \sqrt{3}s_u$) remains constant unless the boundaries are very close. The results suggest that there exists an almost unique A value for each b value which is irrespective of the boundary distance when $b < 0{\cdot}6$ unless the boundaries are close.

ANALYSIS OF PILE RESPONSE USING THE SUBGRADE REACTION METHOD

In the subgrade reaction method of lateral pile design it is inherently assumed that the lateral pressure on the pile at many particular depth is dependent solely on the lateral displacement of the pile at that depth (and the soil properties). This suggests that soil shear in the horizontal plane around the pile due to the relative lateral movement of the pile past the soil dominates the lateral response at any pile depth. This implies that the p–δ curves obtained by analysing the shear

around a disk using 2-D finite element analysis may also describe p–y curves for single piles in undrained conditions[18] although p–y stiffness at shallow depths might be overestimated due to three-dimensional effects.

A finite difference program[19] was written to calculate the response of an elastic pile of length, 1, with bending stiffness, EI, to lateral and moment pile head loads. The soil–pile (p–y) interaction was modelled using the p–δ curves obtained from the 2-D finite element analysis.

The pile equilibrium equation is given below

$$\frac{\mathrm{EI}}{d}\frac{\mathrm{d}^4 y}{\mathrm{d}z^4} + \frac{F}{d}\frac{\mathrm{d}^2 y}{\mathrm{d}z^2} + p = 0 \tag{4}$$

where y is the lateral pile displacement at may given length, z along the pile, F is the pile axial force (assumed to be zero in the analyses presented in this paper as it has little effect on the lateral response for most pile conditions) and the lateral pile pressure, $p = k(y/d)$ where k is the secant p–y/d stiffness for the pile for the given pile displacement and depth. Equation (4) is solved in a finite difference matrix form to obtain $y(z)$ for a given set of pile head loads and boundary conditions and the moment and pile pressure distributions along the pile are calculated. At the pile tip, it is assumed that the moment and shear is zero.

Results from the calculation method are presented later for the geometries studied with finite element analysis to allow direct comparison of the two methods.

THREE-DIMENSIONAL FINITE ELEMENT ANALYSIS

The package CRISP was used for the 3-D finite element modelling. Again, due to symmetry only a section between mid-pile and the mid-way between piles in a row was analysed. The mesh was similar to that used by Bransby and Springman[20] with 740 linear strain elements and 12,895 degrees of freedom. The pile was of diameter, d length 1 and of stiffness E_p. It had a cone at the tip which ensured that there was negligible tip bending moment. To allow later analysis of pile groups, the mesh was configured with another pile behind it. In the analyses reported here, the second 'pile' was given material properties identical to the surrounding soil, thereby only a single pile was modelled.

As during the 2-D analyses, the soil was undrained and described with either linear elastic or a (non-linear) power-law model. This allowed analysis of equivalent soil conditions in the 2-D and 3-D analyses. Pile head loading was applied using displacement control: the pile head was translated laterally. For free-head loading conditions, the rotation of the pile top was unconstrained, whereas for the fixed-head loading conditions, vertical movement and rotation of the top surface of the pile was prohibited.

The pile bending moment profile was obtained from the axial stresses in the pile at the centroids of elements along its length. This allowed determination of moment at eight points and so an approximation of the bending moment profile along the pile could be found. At the same depths, the lateral pile pressure was calculated by summing the normal and shear stresses applied to the pile by the soil immediately surrounding it. The pile displacement profile could be obtained directly from the FE output and so p–y curves could be presented.

Below, 3-D finite elements results are presented for power-law soil before the pile loadings and deflections are compared with those predicted with the subgrade reaction method using the p–δ curves found from the 2-D analysis. The 3-D results are then shown for linear elastic soil.

RESULTS FROM 3-D FINITE ELEMENT ANALYSIS AND THE SUBGRADE REACTION METHOD

Power-law soil

A full three-dimensional finite element analysis was carried out with undrained power law soil with $q = a\varepsilon_q^{0\cdot65}$ and $E_p/a = 21{,}700$. A free-head pile displacement, $y_0/d = 0\cdot157$ was applied and the deformed mesh is shown in Figure 5. The pile is not quite long enough to be considered flexible as there is some rotation and displacement at the pile tip.

Figure 6 shows a horizontal cross-section of the deformed mesh at a depth, $z = 2\cdot44d$. There is significant local shearing of the soil around the pile.

Investigation of strains around the pile at $y_0/d = 0\cdot157$ reveals that at depth $z = 2\cdot44d$, the maximum horizontal strain, $\varepsilon_y = 0\cdot0134 = 0\cdot164$ (y/d) close and in front of the the pile, $\varepsilon_x = 0\cdot0134$ behind the pile (close to the pile, $\varepsilon_y \approx -\varepsilon_x$ because the soil in undrained and $\varepsilon_z \approx 0$), whereas the maximum vertical strain $\varepsilon_z = 0\cdot0036 = 0\cdot044$ (y/d) about one diameter behind the pile. This suggests that the vertical strain is an intermediate principal strain and therefore has little effect on the stress–strain behaviour of the soil as $\gamma_{\max} = |\varepsilon_x - \varepsilon_y|$.

The p–y curves obtained for different depths along the pile are shown in Figure 7. The p–y curves at different depths in the uniform soil are very similar. This is partly due to the homogenous soil properties, but suggests additionally that the p–y behaviour is hardly affected by the proximity to the solid surface or the base of the soil.

The p–δ curve obtained from 2-D FE analysis is also plotted in Figure 7. For the power law exponent, $b = 0\cdot65$ then $A = 3\cdot1$ from Figure 4, and so $p = 3\cdot1\ a(\delta/d)^{0\cdot65}$. The p–δ curve is about 25 per cent stiffer than the p–y curves from the 3-D analysis.

The disparity between the load–transfer curves from the 2-D and 3-D finite element analysis is due to the far field three-dimensional soil displacements. As the pile is pushed into the soil and

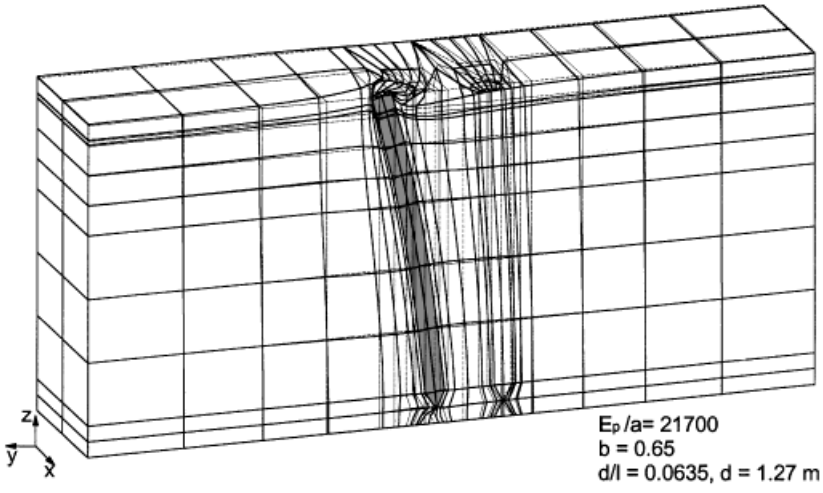

Figure 5. Deformed mesh plot. 3-D analysis of a free-head pile with $y_0 = 0\cdot2$ m

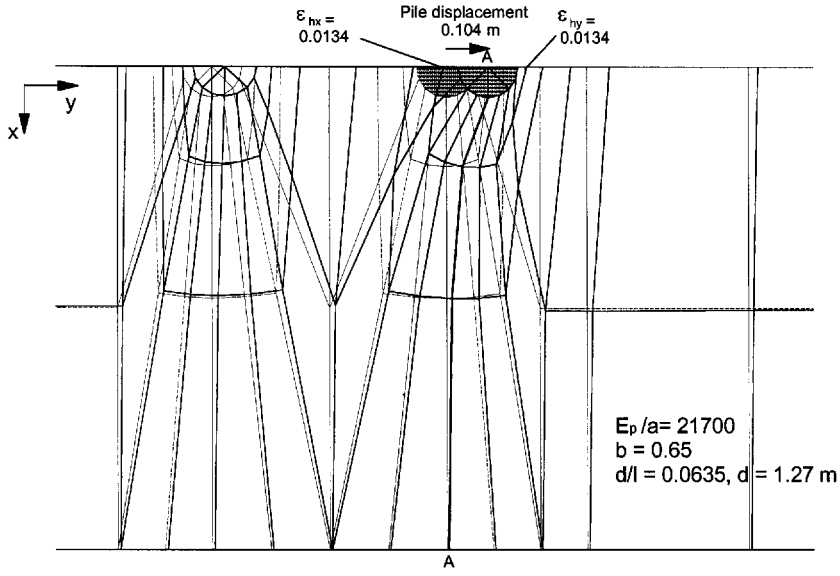

Figure 6. Deformed mesh around pile at $z = 2{\cdot}44$ d

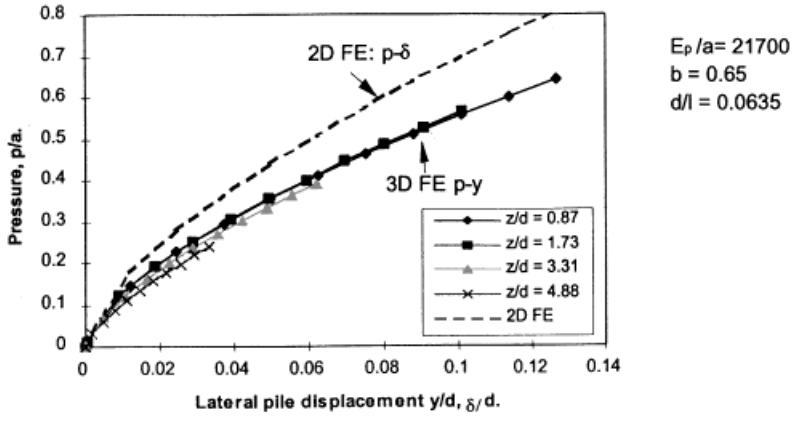

Figure 7. Comparison of p–δ with 3-D FE analysis measured p–y curves

pile pressures develop two things occur. Firstly, there is the local soil shear as the soil resists the movement of the pile through it (this is examined in the 2-D finite element analysis). Secondly, the lateral pile pressure causes far-field soil displacements in the vertical (z–y) plane. In effect these displacements mean that the pile pushes soil along with it. The soil displacements in front and behind the pile are shown in Figure 8 for the vertical plane through the centre-line of the pile in the direction of loading. This suggests that full three-dimensional analysis is required to get the *exact* solution for the p–y curves (which will be pile geometry and fixity dependent). The effect of

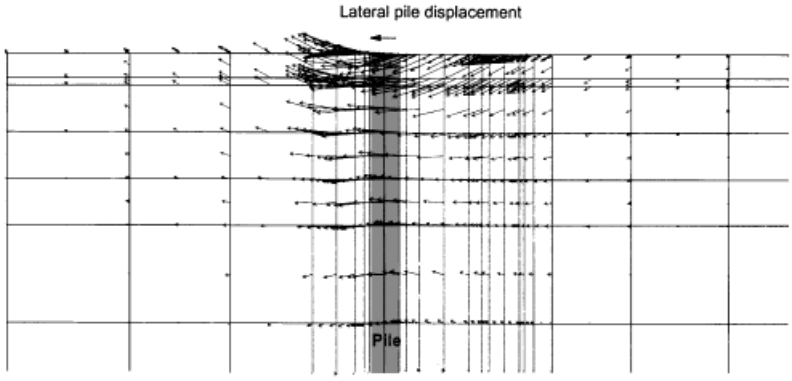

Figure 8. Soil displacements in the vertical plane of the pile centre: 3-D FE

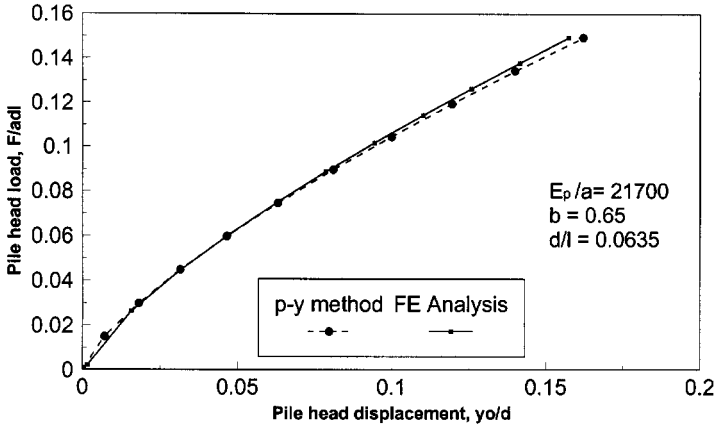

Figure 9. Pile head load–displacement relationship: p–y method 3-D FE

using the two — dimensional p–δ analyses as p–y curves (with the intrinsic error discussed above) in engineering design is investigated below.

Despite the small disparity between the stiffness of the p–y curves and the p–δ curves from the 2-D analysis, an analysis of the pile using the finite difference subgrade reaction program was carried out using the p–δ curves obtained from the plane strain FE analysis as p–y curves. As the pile analysis required pile head loadings as input parameters, the pile head loading from the (displacement controlled) 3-D FE analysis was deduced and applied as the loading condition. The program was then used to calculate the pile head deflection, deflected shape and bending-moment profile and pressure profile for that given head loading.

The pile head load–displacement response is shown in Figure 9 for both the 3-D finite element analysis and the equivalent subgrade reaction method. There is excellent agreement between the two methods. This is a little surprising considering the disparity between the p–δ and p–y curves

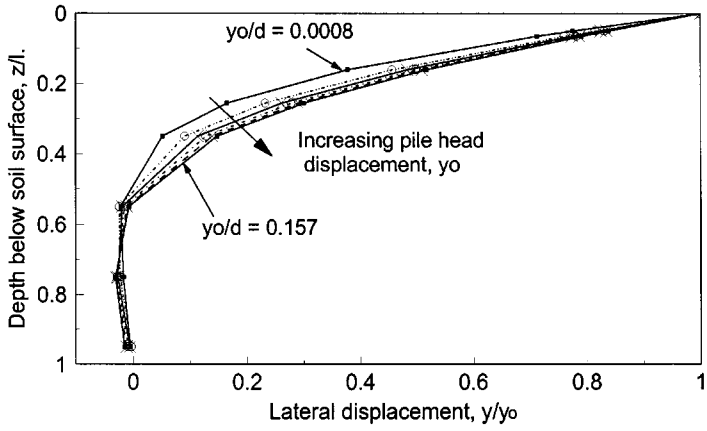

Figure 10. Pile-displacement profile at different head displacements: 3D FE

but perhaps suggests the insensitivity of the subgrade reaction method to the exact form of the p–y curves used.

Figure 10 shows the calculated pile-displacement profile from the 3-D analysis for a range of pile head displacements, y_0/d. It is evident that as the pile displacement increases the pile behaves less flexibly. This is because the secant modulus of the soil reduces with increasing pile displacement because of the induced shear strain, thus increasing the average pile/soil stiffness ratio. The strain softening varies with position around and along the pile and with the pile displacement. Hence, choice of appropriate secant shear moduli for pseudo-elastic characterization of the pile–soil stiffness ratio for any pile displacement would be inapropriate. However, the subgrade reaction model is seen to be able to predict accurately the pile head load–displacement behaviour (Figure 9) for a range of pile-displacement profiles.

Good agreement is obtained by comparing the pile-deflected shape at pile head displacement, $y_0/d = 0{\cdot}157$ (Figure 11) from the two calculation methods. This suggests that the subgrade reaction method predicts well both the shape and the magnitude of the pile deflection due to the head loading.

Figure 12 shows the pile bending-moment profiles obtained from the finite element analysis and the subgrade reaction method. There is good agreement between the results with only a slight under prediction of the peak–bending moment using the p–y method.

The accuracy of this prediction along with the pile displacements suggests that the subgrade reaction method approximates the behaviour of the full three-dimensional problem extremely well and that the slight disparity between the stiffness of the p–y and p–δ curves in this foundation geometry is not critical for design.

Verification of findings for different power law boundary conditions. To check that the findings for the specific case of the free head pile in soil with $b = 0{\cdot}65$ were general, further 3-D FE analyses were carried out for varying soil exponents, b, soil stiffness moduli, a and pile in head-fixity conditions. Figure 13 shows the p–y curves obtained for a pile in power-law soil with $b = 0{\cdot}65$ for both the fixed and free-head conditions The similarity of the p–y curves despite the varying

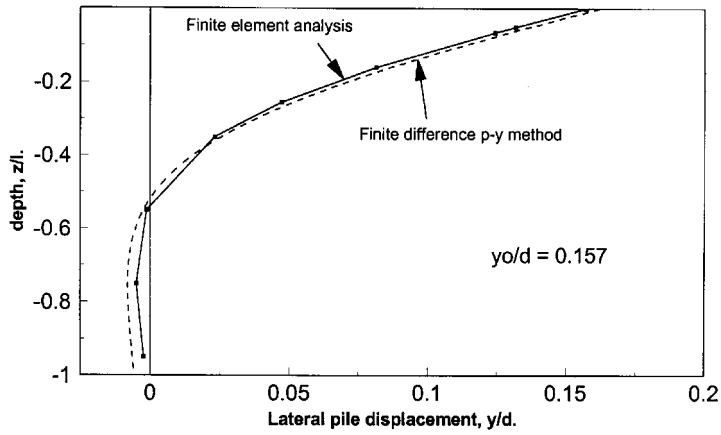

Figure 11. Displaced pile profile: p–y method versus 3D FE

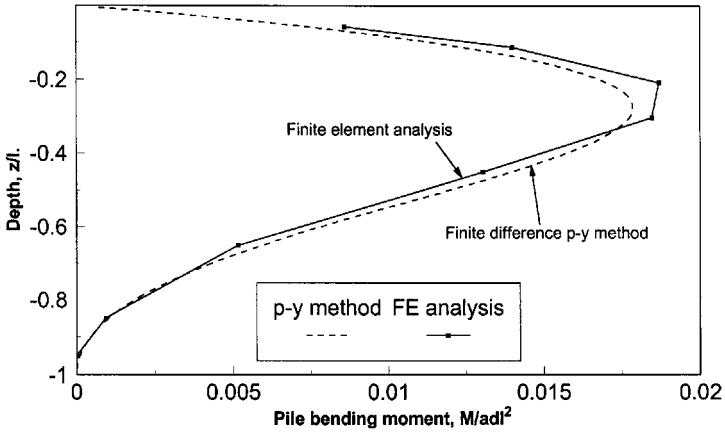

Figure 12. Pile bending moment profile: p–y method versus 3D FE method

pile-displacement profiles (Figure 14) suggests that the head-fixity conditions do not affect the p–y curves significantly.

Figure 15 shows p–y curves from three free-head tests in power-law soil with $b = 0{\cdot}35$. The pile-soil stiffness ratio is varied in the three tests giving $E_p/a = 11{,}667$, $E_p/a = 46{,}669$ and $E_p/a = 116{,}670$. The difference between the deflected profiles is shown in Figure 16 for two pile head displacements showing the difference in pile flexibility between the three tests. From Figure 15 it is apparent that the p–y curves at shallow depths (eg. $z/d < 2$) are similar to the p–δ curves produced from the plane strain analysis for all analyses. Indeed, there is less difference between the p–y curves and the p–δ curves for the soil with $b = 0{\cdot}35$ than for the previous analyses with $b = 0.65$. However, at greater depths the p–y curves become softer. This is especially evident for the more flexible pile ($E_p/a = 11{,}667$) where there is a large amount of bending (and consequently

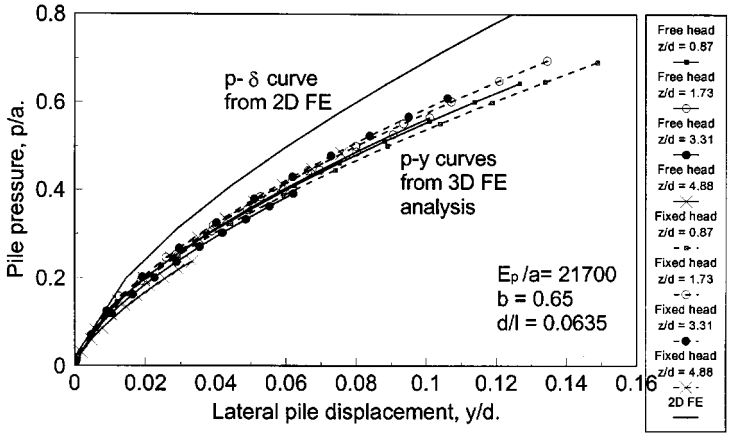

Figure 13. Fixed-head and free-head p–y curves in $b = 0{\cdot}65$ soil

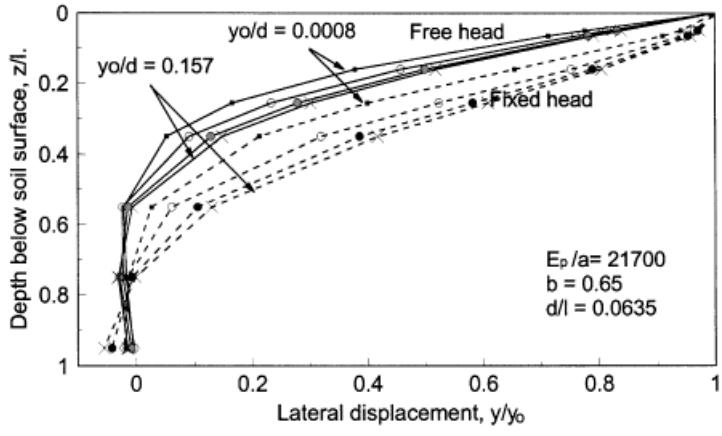

Figure 14. Pile-displacement profile for different head displacements and fixities: 3-D FE

a large variation of displacement and hence pile pressure) near the head of the pile. This suggests that for very flexible piles, interaction along the length of a single pile may not be negligible, and will lead to some p–y softening with increased depth.

Linear elastic soil

Similar (3-D) analyses were carried out for a pile translated through uniform, linearly elastic, undrained material. Three different elastic soil stiffness, G were used in order to investigate the effect of different relative pile–soil stiffness. From Randolph's analysis[6] of single piles in an elastic continuum the characteristic pile length, $1_c = d(E_p/G_c)^{2/7}$, where E_p is the Young's modulus of the pile material for an equivalent solid circular pile and $G_c = G(1 + 3v/4)$ for uniform elastic

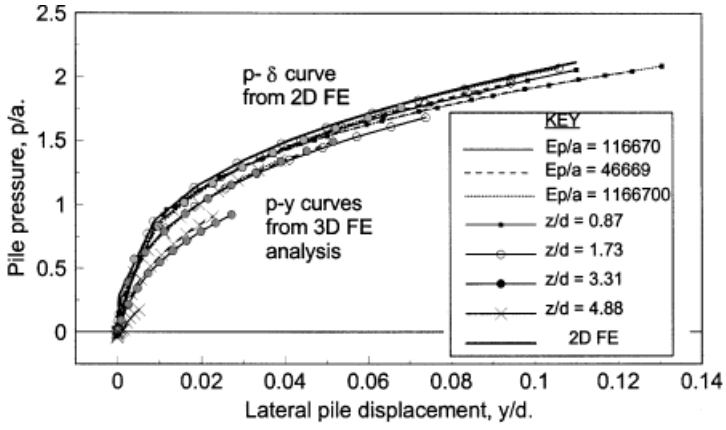

Figure 15. p–y curves for pile in $b = 0{\cdot}35$ soil

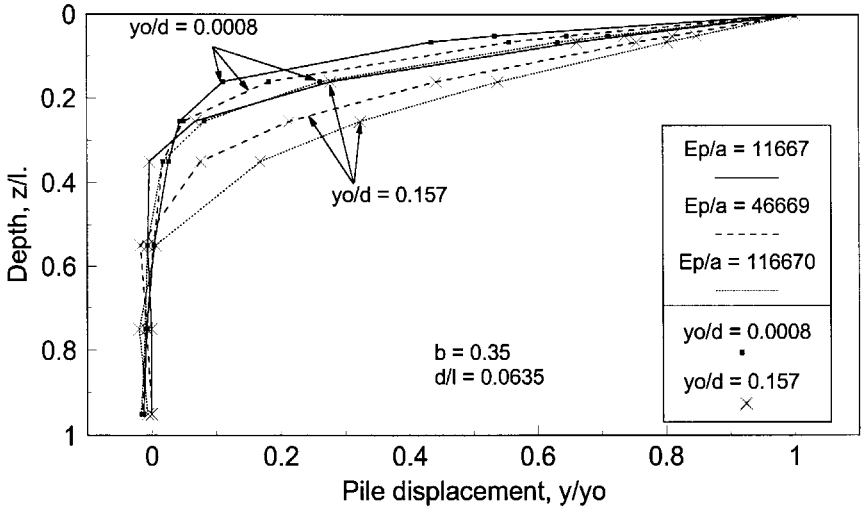

Figure 16. Deflected pile profiles in $b = 0{\cdot}35$ soil with varying relative pile stiffness: 3-D FE results for two different pile head displacements.

material. For the undrained conditions considered here, the soil and pile conditions gave non–dimensional pile lengths, $l/l_c = 3{\cdot}033$, $2{\cdot}488$ and $2{\cdot}03$, respectively.

Both free-head and fixed-head translation of the pile head was applied, displacing the pile by a distance y_o and the pile displacement, loading and moment profiles were determined. The pile-deflection profiles obtained (Figure 17) show that in all soils, the pile behaved flexibly as would be expected with $l/l_c > 1$.

The load–transfer curves (shown for a free-head pile with $l/l_c = 2{\cdot}03$ in Figure 18) revealed that the p–y stiffness reduces with depth. The gradient is presented as a multiple of the soil stiffness and

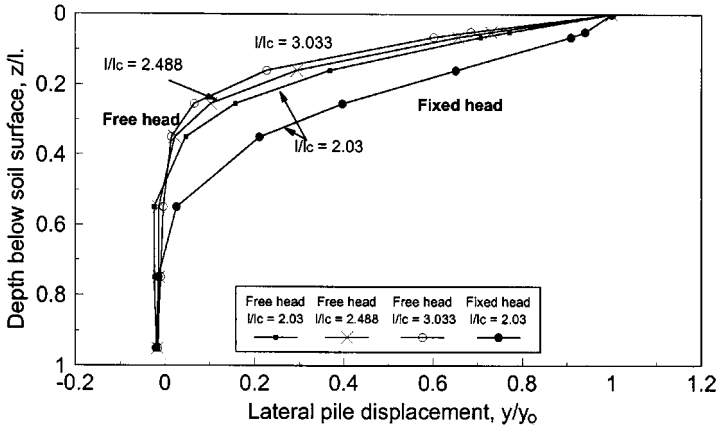

Figure 17. Pile defection profiles: 3-D FE analysis, linear elastic soil

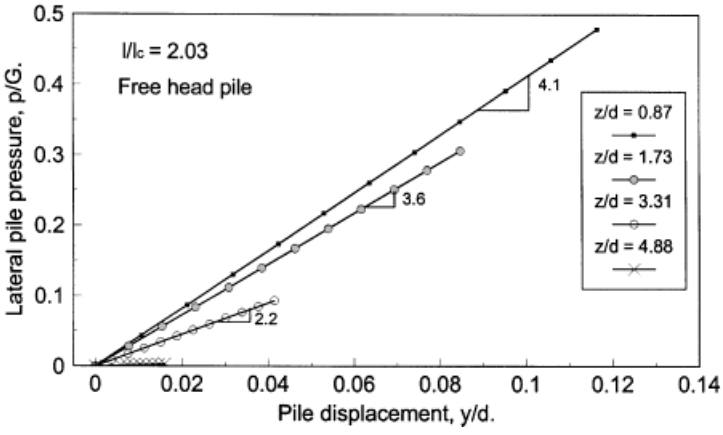

Figure 18. p–y curves: 3-D FE analysis, linear elastic soil

plotted on Figure 19 as the dimensionless constant, $3A = p/((y/d)G)$ which is derived from the power law equation (3): $p = A3\mathrm{G}(y/d)$ ($a = 3G$ for a linear power law). In all load cases, A reduces with depth and this varies by different amounts depending on the mode of pile deformation. However, for all cases $3A \approx 4{\cdot}1$ at $z = 1$ m, a slightly surprising result given that surface effects would be expected to reduce the p–y stiffness at small depths.

The p–y stiffness behaviour is very different to that observed for the power law soil where the p–y curves were almost unaffected by the depth along the pile. Indeed, for the elastic case, the stiffness of the p–y curves (Figures 18 and 19) reduce with depth along the pile, this despite the fact that the actual soil stiffness is independent of depth. This behaviour was also observed for a wider range of pile conditions by Baguelin and Frank.[21] The reduction in stiffness must be due to far-field soil displacements which do not reduce significantly away from the pile especially in the

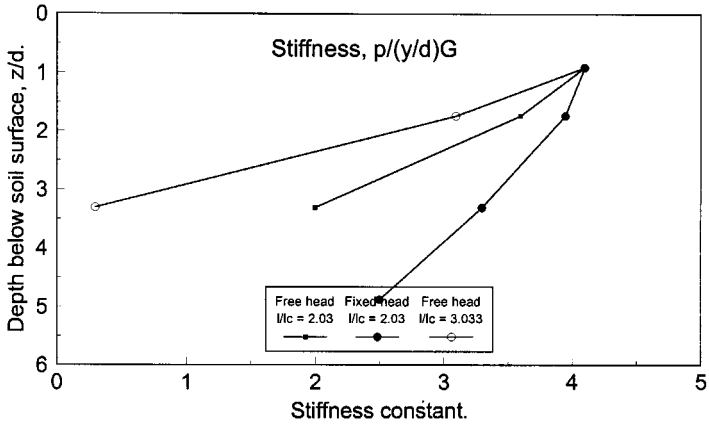

Figure 19. Elastic stiffness constant with depth. 3-D FE, free- and fixed-head piles

horizontal plane.[12] This ensures that significant three-dimensional soil displacements occur which cause the p–y response at any one depth to be affected significantly by load and displacements elsewhere along the pile. Indeed, at large depths it is possible that negative p–y gradients result as the 3-D continuum displacements become larger than pile displacements and so a type of passive lateral loading results.

DISCUSSION

Unexpectedly, it appears that the choice of p–y curves for representation of the behaviour of single piles translated laterally though linearly elastic, homogeneous soil is more complex than those translated through non-linear, power-law soil. The reason is that far-field soil displacements are very significant for the linear-elastic case and so the 3-D effects are important. However, in the case of power law with $b < 1$, soil displacements remote from the pile reduce quickly and so the three-dimensional effects become less significant unless the pile is very flexible. When 3-D effects are insignificant, p–y curves may be predicted solely from 2-D analyses thus allowing simple design methods and suggesting that there are almost unique p–y curves, independent of pile-displacement conditions, for any power-law soil stress–strain curve.

There is no such thing as a unique *elastic* p–y stiffness: the stiffness varies with depth and pile head-loading condition even in uniform soil.[21] Therefore choice of p–y stiffness cannot be made just through consideration of the characterization of soil with elastic properties as done routinely in design. Instead, an average stiffness factor $(p/(G(y/d)))$ must be chosen (perhaps using the recommendations of Baguelin *et al.*[21]) which will give the best response for the pile head displacement and maximum pile moment when used in a subgrade reaction analysis. However, near the surface all the pile cases investigated gave a unique value of $p/(G(y/d)) \approx 4{\cdot}1$ although use of this value for analysis will lead to non-conservative estimates of pile head deflection for most pile geometries.

Real soil is non-linear even at very small strains ($\gamma > 10^{-4}$). This means that (non-linear) p–y curves obtained from field or laboratory tests are not likely to be dominated by far-field soil displacements and so will be almost independent of pile head-fixity conditions.[1,9,22] It is likely

that the p–y curves may be predicted from the equivalent 2-D p–δ curves which are unique for given soil conditions.

IMPLICATIONS FOR DESIGN

For soils which can be described by a power law, the excellent agreement between results from the 3-D finite element analysis and the subgrade reaction method of analysis using the 2-D finite element derived p–δ curves as p–y curves suggests that this will form the basis of a suitable design method for single piles. Although the p–δ analysis ignores effects such as out-of-plane deformation and soil shear between different depths, the similarity of the p–δ curves to the p–y curves suggests that these effects are often small.

A serviceability design method is recommended using the 2-D power-law pile analyses together with the subgrade reaction method. For every depth, the factor for power-law scaling, A would be found using the A–b relationship presented for pile translation through undrained power-law soil (Figure 4) following characterization of the soil with power-law parameters a and b. Once A, a and b are found at every depth, the p–y curve at the depth can be calculated using a modified form of equation (3):

$$p = Aa\left(\frac{y}{d}\right)^b \tag{5}$$

The p–y curves at every depth can then be input to the subgrade reaction method which would allow prediction of undrained serviceability pile behaviour for different boundary conditions and pile geometries.

This method is similar to the empirically derived p–y recommendations by Wesselink *et al.*[4] for calcareous sand, in which the p–y equation is characterized by

$$p = R\left(\frac{z}{z_o}\right)^N\left(\frac{y}{d}\right)^\gamma \tag{6}$$

where R is a stiffness modulus, z_o is a reference depth and N and γ are exponents chosen to describe the change in p–y stiffness with depth and pile displacement, respectively. This method has recently been shown to give good results for calcareous silt[9] and is likely to be suitable for a range of soils and loading rates at pre-failure pile displacements after empirical choice of variables R, N and γ. Indeed, preliminary analysis of results by Dyson[23] suggests that empirically derived values of γ agree with values of power-law exponent, as determined from soil-element testing.

CONCLUSIONS

(1) Two-dimensional and three-dimensonal finite element analysis was carried out of a single-pile subject to lateral head loading in both undrained power-law soil and linear elastic soil.
(2) For the case of an undrained soil able to be described by a power law, $q = a\varepsilon_q^b$, the p–y curve was found to be almost independent of pile head loading or boundary conditions and therefore almost unique for a given soil stress–strain law. This meant that by use of the subgrade reaction method of lateral pile analysis, the 3-D finite element results could be replicated using the load–transfer curves obtained with the 2–D finite element analysis. This

suggests that this approach will form a good design method, allowing prediction of p–y curves from fundamental soil properties and deformation behaviour.

(3) A methodology is presented for the selection of p–y curves for undrained, serviceability pile behaviour using the 2-D power-law pile analysis for input into the subgrade reaction method. Input p–y curves for the subgrade reaction method are calculated with equation (5) using Figure 4 as a design chart for selection of A following the characterization of the soil as a power law.

(4) The p–y curves found in the 3-D finite element analysis were softer than the p–δ curves obtained for the same soil using plane strain analysis. This is due to the three-dimensional far-field displacements which soften the p–y response. This softening is small for single piles or widely spaced pile rows in power law soil unless the pile is very flexible, but it will need to be considered for pile groups[18] or for linear elastic soil.

(5) For linearly elastic undrained soil, there was not a unique p–y curve stiffness for any given soil stress–strain law (shear modulus). Instead, the p–y stiffness varied with pile head-loading conditions and pile regidity as already shown by Baguelin and Frank.[21] This was because the linearity of the soil stress–strain law and the undrained soil behaviour caused the far-field three-dimensional soil displacements to become significant. Instead, to use elastic p–y curves to predict pile head displacements even in a true linear elastic medium (not a likely soil condition), an average relationship between the p–y curve stiffness and the shear modulus must be chosen which is dependent on pile geometry and loading conditions.[12,21]

ACKNOWLEDGMENTS

The work described forms part of the activities of the Special Research Centre for Offshore Foundation Systems, funded through the Australian Research Council's Research Centres Program.

The Author would like to thank Professor Mark Randolph and Gerard Dyson from UWA for useful discussion of the above work and the referees for their useful comments.

APPENDIX: NOTATION

a	power-law constant
A	power-law scaling constant
b	power-law exponent
d	external pile diameter
E_p	Young's modulus of the pile
I	second moment of area of the pile
G	shear modulus of soil
l	pile length
l_c	characteristic pile length (after Randolph[6])
p	lateral pile pressure
p_u	ultimate lateral pile pressure
q	deviatoric stress
R	distance from pile centre to rigid boundaries
s_u	undrained shear strength

s_x pile spacing along the pile row
x,y Cartesian co-ordinate system
y lateral pile displacement
y_0 lateral pile head displacement
z depth below top surface of soil
δ lateral pile displacement in 2-D
ε_q deviatoric strain

REFERENCES

1. H. S. Matlock and L. C. Reese, 'Generalised solutions for laterally loaded piles', *J. Geotech Engng. Div., ASCE* **86**(5), 63–91 (1960).
2. W. R. Sullivan, L. C. Reece, and C. W. Fenske, 'Unified method for analysis of laterally loaded piles in stiff clay', *Numerical Methods in Offshore Piling*, ICE, London (1980) pp. 135–146.
3. American Petroleum Institute, Recommended practice for planning. designing and constructing fixed offshore platforms, 17th edn, *IAP-RP2A*, A.P.I., Washington, 1987.
4. B. D. Wesselink, J. D. Murff, M. F. Randolph, I. L. Nunez and A. M. Hyden, 'Analysis of centrifuge model test data from laterally loaded piles in calcareous sand', *Engineering for Calcareous Sediments*, Vol. 1, Balkema, Rotterdam, (1988) pp. 261–270.
5. H. G. Poulos, 'Behaviour of laterally loaded piles: I-single piles, and II-pile groups', *JSMFD, ASCE* 97, **SM5** 711–731, 733–751 (1971).
6. M. F. Randolph, 'The response of flexible piles to lateral loads', *Geotechnique* **31** (2), 247–259 (1981).
7. Y. O. Barton, W. D. L. Finn, R. H. G. Parry and I. Towhata, 'Lateral pile response and p–y curves from centrifuge tests', 15*th OTC*, Houston, Texas, 1983.
8. L. Yan, P. M. Byrne 'Lateral pile response to monotonic pile head loading', *Can Geotech. J.* **29**, 955–970 (1992).
9. G. J. Dyson and M. F. Randolph, 'Load-transfer curves for piles in calcareous sand', *Proc. 8th Int. Conf. on the Behaviour of Offshore Structures, Delft, July* 1997, Vol 3, 1997, pp. 245–258.
10. H. S. Matlock, 'Corrrelations for design of laterally loaded piles in soft clay', 2*nd Annual Offshore Technology Conf. Houston, Paper OTC 1204*, 1970.
11. M. Yegian and S. G. Wright, 'Lateral soil resistance-displacement relatioships for pile foundations in soft clays', *5th Annual Offshore Technology Conf. Houston, Paper OTC 1893*, Vol. 2, 1973, pp. 663–676.
12. F. J. Baguelin,. R. A. Frank and Y. Said, 'Theroretical study of lateral reaction mechanism of piles', *Géotechnique* **27**(3), 405–434 (1977).
13. R. D. Mindlin, 'Force at a point in the interior of a semi-infinite solid', *Physica*, **7**, 195–202 (1936).
14. M. F. Bransby and S. M. Springman, 'Development of lateral deformation mechanisms around a pile', *Proc. NUMOG V, Davos*, 1995, pp. 607–612.
15. A. M. Britto and M. J. Gunn, *Critical State Soil Mechanics via Finite Elements*., Ellis Horwood Ltd, Chichester, 1987.
16. A. M. Britto and M. J. Gunn, *CRISP90. User's and Programmer's Guide*, 1990.
17. H. Winter and A. Hettler, 'Ähnlichkeit bei Randwerproblemen und ihre andwendung in Sandmechanik', *Ing.-Archiv.* **53,** 27–39 (1982).
18. M. F. Bransby, 'Difference between load-transfer relationships for laterally loaded pile groups: active p–y or passive p–δ', *J. Geotech. Egng ASCE*, **122**(12)**,** 1015–1018 (1996).
19. M. F. Bransby, Piled foundations adjacent to surcharge loads, *Ph.D. Thesis*, University of Cambridge, 1995.
20. M. F. Bransby and S. M. Springman, '3-D finite element modelling of pile groups adjacent to surcharge loads', *Comput. Geotech*, **19** (4), 301–324 (1996).
21. F. J. Baguelin and R. A. Frank, 'Theoretical studies of piles using the finite element method', *Numerical Methods in Offshore Piling*, ICE, London, 1980, pp. 83–91.
22. W. G. K., Fleming, A.J. Weltman, M.F. Randolph and W. K. Elson, *Piling Engineering* (2nd edition) Blackie Academic & Professional, Glasgow, 1992.
23. G. J. Dyson, 'Obtaining cyclic load-transfer curves', *ANZ Young Geotechnical Proffessional Conf. Melbourne, Australia*, 1998.

